

# Cationic Effect on Pressure driven Spin-State Transition and cooperativity in Hybrid Perovskites

Hrishit Banerjee,<sup>†</sup> Sudip Chakraborty,<sup>‡</sup> and Tanusri Saha-Dasgupta<sup>\*,†</sup>

*Department of Condensed Matter Physics and Material Sciences, S N Bose National Centre for Basic Sciences, and Materials Theory Division, Department of Physics and Astronomy, Uppsala University, Box 516, 75120 Uppsala, Sweden*

E-mail: t.sahadasgupta@gmail.com

## Abstract

Hybrid or metal organic framework (MOF) perovskites of general composition,  $ABX_3$ , are known to show interesting properties which can lead to variety of technological applications. Our first principles study shows they are also potential candidates for exhibiting cooperative spin-state transitions upon application of external stimuli. We demonstrate this by considering two specific Fe-based MOF perovskites, namely Dimethylammonium Iron Formate,  $[\text{CH}_3\text{NH}_2\text{CH}_3][\text{Fe}(\text{HCOO})_3]$  and Hydroxylammonium Iron Formate,  $[\text{NH}_3\text{OH}][\text{Fe}(\text{HCOO})_3]$ . Both the compounds are found to undergo high-spin ( $S=2$ ) to low-spin ( $S=0$ ) transition at Fe(II) site upon application of moderate strength of hydrostatic pressure, along with large hysteresis. This spin-state transition is signaled by the changes in electronic, magnetic and optical properties. We find both the transition pressure and the width of the hysteresis to be strongly dependent of the choice of A-site cation, Dimethylammonium or Hydroxylammonium, implying tuning of spin-switching properties achievable by chemical variation of the amine cation

---

\*To whom correspondence should be addressed

<sup>†</sup>Department of Condensed Matter Physics and Material Sciences, S N Bose National Centre for Basic Sciences

<sup>‡</sup>Materials Theory Division, Department of Physics and Astronomy, Uppsala University, Box 516, 75120 Uppsala, Sweden

in the structure. Our finding opens up novel functionalities in this family of materials of recent interest, which can have important usage in sensors and memory devices.

## Introduction

Metal organic framework compounds, built from inorganic and organic components, form an active area of research which has undergone a rapid growth in last decade.<sup>1,2</sup> Bulk of the study in this field are focused on open systems with large porous region having potential applications in gas storage,<sup>3</sup> chemical sensing,<sup>4</sup> catalysis<sup>5</sup> etc. In recent time attention has been given also to dense hybrid frameworks with limited porosity. Some of these dense hybrid compounds adopt the celebrated perovskite geometry of general formula  $ABX_3$ .<sup>6</sup> This has opened up an emerging research area on hybrid perovskites, parallel to the well-established field of inorganic perovskite oxides. The halide hybrid perovskites of general composition,  $[AmH]MX_3$  ( $AmH^+$  = protonated amine,  $M = Sn^{2+}$  or  $Pb^{2+}$ , and  $X = Cl^-$  or  $Br^-$  or  $I^-$ ) have already attracted great deal of attention due to their potential use in solar cell applications.<sup>7</sup> The other class of hybrid perovskites discussed in very recent time due to their attractive ferroic properties, are transition metal formates  $[AmH]M(HCOO)_3$  ( $M = Mn, Cu, Ni, Fe, Co$ ), where  $MO_6$  octahedra are linked via formate bridges, and the protonated amine molecules sit in the hollow formed by the octahedral framework, establishing hydrogen bonding with formates.<sup>8</sup> The presence of organic components in the structure offers greater structural flexibility, and thus better tunability of properties by external means, as compared to that of inorganic perovskites. The flexibility of hybrid perovskite to undergo large structural changes in response to external stimuli has been already reported.<sup>9</sup> Furthermore, it is possible to tailor properties by changing the amine molecule, thereby changing the strength and cross-linking of hydrogen bondings in the structure, yet maintaining the basic topology.<sup>10</sup> Needless to say, much remains to be explored in terms of functionalities that can be achieved in this new class of perovskite materials.

In this study, we focus on one such unexplored area, namely the external stimuli driven spin-

crossover (SCO). The tremendous flexibility of the organic linkers makes the transition metal based formate hybrid perovskites ideally suited for triggering spin-crossover from a high-spin (HS) to low-spin (LS) state at the transition metal site by external perturbation. A much discussed aspect in this context is the issue of cooperativity in SCO phenomena.<sup>11</sup> The cooperativity in SCO phenomena makes it a spin transition rather than spin-crossover, which may show up with associated hysteresis, having important implications in designing memory devices.<sup>12</sup> For device applications, the challenge is to make the width of the hysteresis large for obtaining the memory effect over a wide range of external stimuli as well as transition to occur at a value of the stimuli that is readily achievable. In this respect, commonly explored candidates are SCO polymers or 3D coordination compounds which are expected to provide better connectivity compared to molecular crystals with isolated molecular units.<sup>13</sup> Considering the dense topology of the newly discussed hybrid perovskites, they can be a potential alternative to SCO polymers or 3D coordination compounds in exhibiting cooperative spin-state transitions. This will add novel functionality in this novel and interesting class of compounds.

In light of the above, we venture on the study of SCO properties of transition metal based formate hybrid perovskites, through first-principles calculations. In particular we consider Fe<sup>2+</sup> based hybrid perovskites. The choice is prompted by the fact that SCO transitions in Fe(II)-based compounds, having 6 *d*-electrons in Fe(II) ion, and showing a transition from a LS ( $S = 0$ ) to a HS ( $S = 2$ ) state are pronounced and abrupt, making them suitable for applications. In our study, we consider hydrostatic pressure as an external stimuli. To the best of our knowledge, no study exists so far on the pressure effect on hybrid perovskites, although hydrostatic pressure is considered as one of the effective means to tune properties in inorganic perovskites.<sup>14</sup> Additionally, to study the influence of changing the primary organic component, namely the amine cation, located in the perovskite cavity, we consider two different cations, Dimethyl-ammonium (CH<sub>3</sub>NH<sub>2</sub>CH<sub>3</sub>), and Hydroxylamine (NH<sub>3</sub>OH). It is worth to note that our conscious choice of these two different molecular cations, leads to a change in the tolerance factor of the Fe formate perovskite structures, as the effective molecular radii for Dimethyl-ammonium and Hydroxylamine are different, being

272 pm and 215 pm, respectively. As was pointed by Kieslich and co-workers,<sup>1</sup> change in mechanical properties, particularly in rigidity can be achieved by changing cations of different effective molecular radius.

Our density functional theory (DFT) based computational study that takes into account all structural and chemical aspects in full rigor, shows that pressure induced spin-state transitions are achieved in both Dimethyl-ammonium Iron Formate (DMAFeF) and Hydroxylamine Iron Formate (HAFeF) compounds for modest critical pressure range of 2-7 GPa, associated with large hysteresis of 2-5 GPa. The latter implies that these compounds should exhibit spin-switchability over a wide range of operating pressure. Our findings highlight the possible technical use of spin-switching functionalities of hybrid perovskite compounds with accompanied changes in electronic, magnetic and optical properties, in sensors and memory devices. Interestingly, the flexibility in choice of the A site cation, *i.e.* the protonated amine molecule adds another dimension, namely the tuning and modulation of spin-switching properties.

## Computational Methodology

Our first-principles calculations were carried out in the plane wave basis as implemented in the Vienna Ab-initio Simulation Package (VASP)<sup>15,16</sup> with projector-augmented wave (PAW)<sup>17</sup> potential. The exchange-correlation functional was chosen to be that of generalized gradient approximation (GGA) implemented following the Perdew-Burke-Ernzerhof<sup>18</sup> prescription. For ionic relaxations, internal positions of the atoms were allowed to relax until the forces became less than 0.005 eV/Å<sup>0</sup>. Energy cutoff of 500 eV, and  $4 \times 4 \times 2$  Monkhorst-Pack k-points mesh were found to provide a good convergence of the total energy in self-consistent field calculations. To take into account of the correlation effect at Fe sites beyond GGA, which turn out to be crucial for the correct description of the electronic and magnetic properties, calculations with supplemented Hubbard U (GGA + U) a la Liechtenstein et al<sup>19</sup> were carried out, with the choice of  $U = 4$  eV and Hund's coupling parameter  $J_H = 1$  eV. In order to study the effect of hydrostatic pressure, calculations

were done by first changing the volume of the unit cell isotropically and then relaxing the shape of the cell together with the ionic positions. The estimate of applied hydrostatic pressure for each compressed volume was obtained from the knowledge of the calculated bulk modulus. The bulk modulus was calculated by varying the volume of the unit cell and relaxing the ionic positions at each volume. Accurate self-consistent-field calculations were carried out to obtain the total energy of the systems at each volume. The energy versus volume data was fitted to the third order Birch-Murnaghan isothermal equation of state,<sup>20</sup> given by,

$$E(V) = E_0 + \frac{9V_0B_0}{16} \left\{ \left[ \left( \frac{V_0}{V} \right)^{2/3} - 1 \right]^3 B'_0 + \left[ \left( \frac{V_0}{V} \right)^{2/3} - 1 \right]^2 [6 - 4 \left( \frac{V_0}{V} \right)^{2/3}] \right\}$$

where  $V_0$  is the equilibrium volume,  $B_0$  is the bulk modulus and is given by  $B_0 = -V(\delta P/\delta V)_T$  evaluated at volume  $V_0$ .  $B'_0$  is the pressure derivative of  $B_0$  also evaluated at volume  $V_0$ .

## Results and Discussions

**Crystal Structure of DMAFeF and HAFeF-** As essential pre-requisite for the first-principles study is the accurate information of the crystal structure. An interesting feature of  $[\text{AmH}]\text{M}(\text{HCOO})_3$  compounds is the order-disorder transition of the A-site amine cations through ordering of hydrogen bonds.<sup>8</sup> While the crystal structure data for disordered phase of DMAFeF<sup>8</sup> is available, no such data exists for the corresponding ordered phase. Moreover, in case of HAFeF, no crystal structure data has been reported till date. Therefore we started with crystal structure data for the ordered phases of DMAMnF<sup>21</sup> and HAMnF,<sup>22</sup> the Mn analogues of DMAFeF and HAFeF. We relaxed the structure completely after replacing Mn atoms with Fe atoms, which gave the first-principles predicted ordered structures of DMAFeF and HAFeF. Mn being next to Fe in the periodic table, this forms a legitimate approach. We carried out a complete structural relaxation, which involved relaxation of the unit cell volume and shape, as well as atomic positions. We found that though the symmetries do not change between Fe compounds and their corresponding Mn counterparts, there is appreciable change in the volume of the unit cells, as expected. DMAFeF and HAFeF crystallize

in two different monoclinic space groups, DMAFeF being in  $Cc$  space group and HAFeF being in  $P2_1$  space group. The lattice constants for DMAFeF are found to be,  $a=14.464\text{\AA}$ ,  $b=8.355\text{\AA}$ ,  $c=8.975\text{\AA}$ , with the angle  $\gamma = 119.8^\circ$ , whereas for HAFeF the lattice constants are found to be  $a=7.812\text{\AA}$ ,  $b=7.961\text{\AA}$ ,  $c=13.173\text{\AA}$ , with angles  $\alpha = \beta = \gamma = 90^\circ$ . The calculated crystal structures as .cif files can be found in the supplementary information (SI).

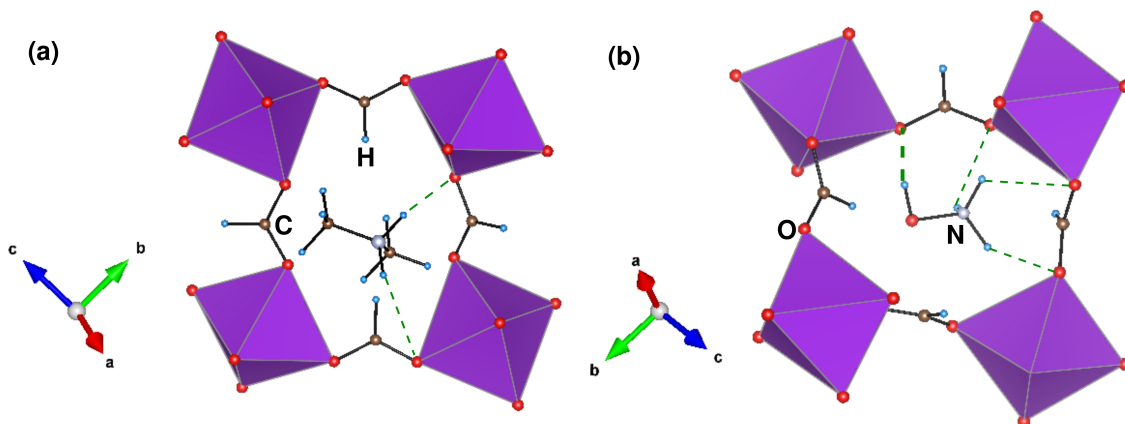


Figure 1: Computed crystal structures of DMAFeF [panel (a)] and HAFeF [panel (b)] in A-site ordered phase. The  $\text{FeO}_6$  octahedra are connected to each other by the formate ligands while the DMA or HA cation sit in the hollow formed by the octahedra. Various atoms have been marked.  $\text{N-H} \cdots \text{O}$  and  $\text{O-H} \cdots \text{O}$  bonds are represented by dashed lines, with thickness of lines indicating the strength of the bonds.

As shown in Fig. 1, in both the framework compounds each  $\text{FeO}_6$  octahedra is connected to neighboring  $\text{FeO}_6$  octahedra via  $\text{HCOO}$  ligand bridges. This forms a three-dimensional  $\text{ReO}_3$ -type network, with Dimethyl-ammonium or Hydroxylamine cations occupying the centers of the  $\text{ReO}_3$ -type cavities. In DMAFeF, two bridging  $\text{N-H} \cdots \text{O}$  hydrogen bonds from each DMA cation are formed, while in HAFeF, three  $\text{N-H} \cdots \text{O}$  hydrogen bonds, and a  $\text{O-H} \cdots \text{O}$  hydrogen bond are formed from each HA cation. The nature of hydrogen bondings is expected to be different between  $\text{N-H} \cdots \text{O}$  and  $\text{O-H} \cdots \text{O}$  due to the less polar nature of  $\text{N-H}$  bond as compared to  $\text{O-H}$  bond. Thus the  $\text{O-H} \cdots \text{O}$  hydrogen bond is stronger than  $\text{N-H} \cdots \text{O}$  hydrogen bond. The lattice for HAFeF is therefore expected to be more rigid compared to the lattice for DMAFeF, having important bearing on SCO phenomena as we will discuss in the following.

**Spin-state transition under pressure and Cooperativity-** In order to determine the spin-

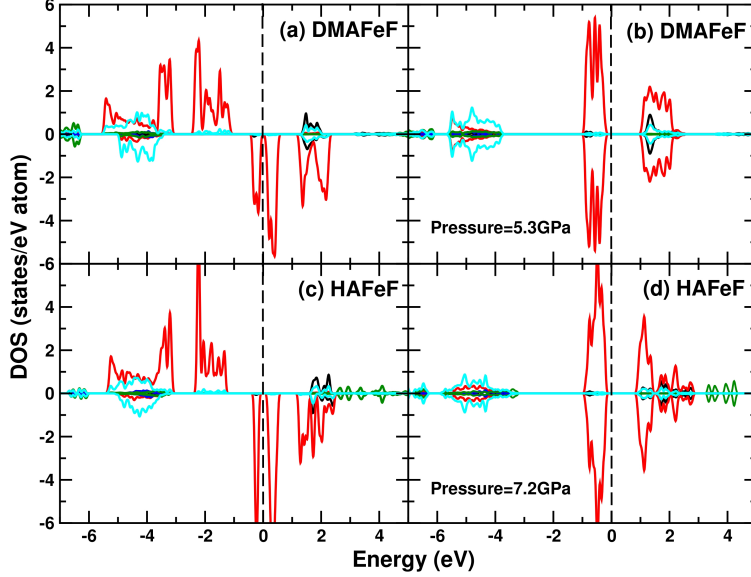


Figure 2: Projected density of states of DMAFeF and HAFeF at ambient and high pressure conditions. Panels (a) and (c) are for ambient pressure, while panels (b) and (d) are for high pressure. The DOS projected to Fe  $d$ , O  $p$ , C  $p$ , N  $p$  and H  $s$  are marked in red, cyan, black, green and blue, respectively. The zero of the energy is set at Fermi energy.

states of the Fe atoms in DMAFeF and HAFeF, we calculated the spin-polarized electronic structures. The spin-polarized density of states at ambient pressure condition for DMAFeF and HAFeF are shown in panels (a) and (c) of Fig. 2, respectively. The states close to Fermi level ( $E_F$ ) are dominantly of Fe  $d$  character, which are found to be strongly spin-polarized. The octahedral coordination of oxygens atoms around Fe, groups the Fe  $d$  states into states of  $e_g$  and  $t_{2g}$  symmetries. The Fe  $d$  states are found to be completely occupied in the majority spin channel, with empty Fe  $e_g$  states, and partially filled Fe  $t_{2g}$  states in the minority spin channel. The distortion in the FeO<sub>6</sub> octahedra causes further splitting within states of Fe  $t_{2g}$ , leading to a small gap at the Fermi region in the minority spin channel. The insulating solution is obtained for both compounds at ambient condition, with a large band gap ( $\approx 2$  eV) between occupied Fe  $d$  and empty C  $p$  states in majority spin channel and a tiny band gap ( $\approx 0.1$  eV) within the Fe  $t_{2g}$  states in the minority spin channel. This suggests at ambient condition spin-state of Fe in both DMAFeF and HAFeF to be HS. The calculated total magnetic moment ( $M$ ) turned out to be  $4 \mu_B$  per Fe atom, for both the compounds, in conformity with the stabilization of HS ( $S=2$ ) state of Fe. Panels (b) and (d) of Fig. 2 show the

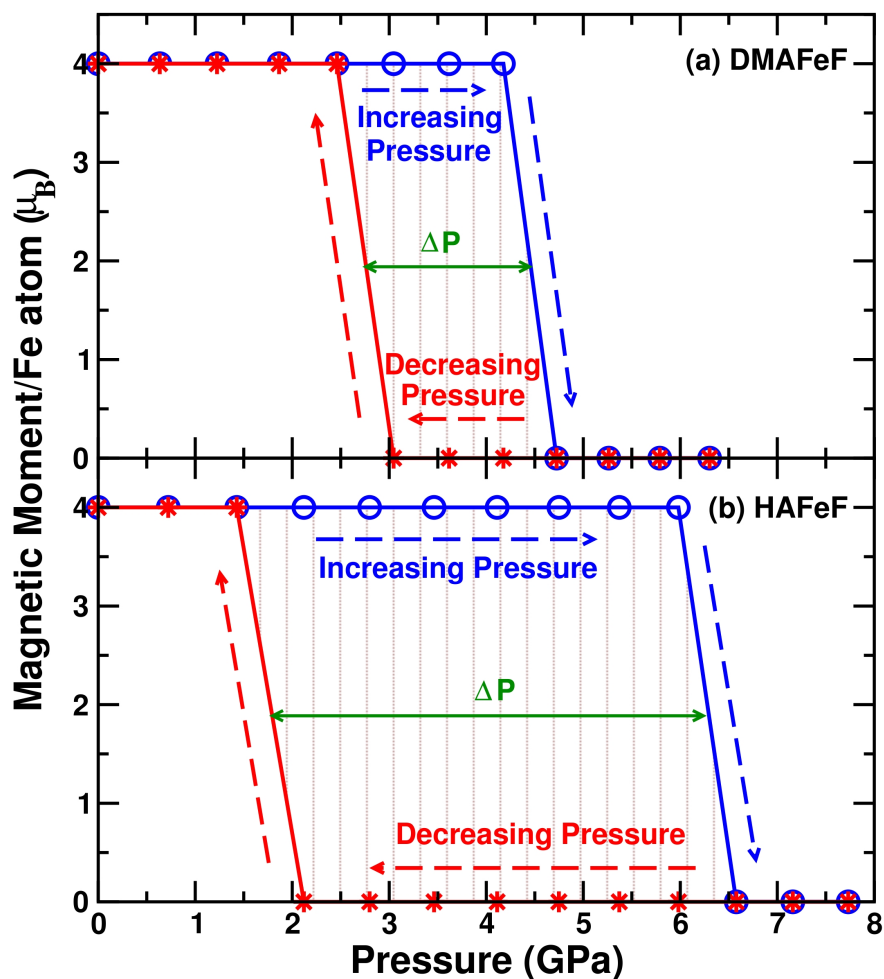


Figure 3: Computed magnetic moment at the Fe site plotted as a function of pressure for DMAFeF [panel (a)] and HAFeF [panel (b)]. The data are plotted for two different paths. The data points in blue denote the path following increasing pressure, starting from the HS state and the data points in red denote the path following decreasing pressure, starting from the LS state. HS  $\rightarrow$  LS transitions in both compounds exhibit interesting hysteresis effects.



spin-polarized density of states for DMAFeF and HAFeF at high pressure condition. We find the exerting pressure (P) in the range of  $\approx 5-7$  GPa causes drastic change in the electronic structure. First of all, for both the compounds the ground states turned out to be non spin-polarized, with calculated magnetic moments of  $0 \mu_B$ . This confirms a spin-state transition from HS (S=2) state to LS (S=0) state, obtained by application of pressure. In the high-pressure LS state a large band gap of  $\approx 1$  eV opens up between the fully occupied Fe  $t_{2g}$  states, and completely empty Fe  $e_g$  states. The spin-state transition thus should be accompanied by a significant change in the over all band gap, which should be manifested in corresponding change in optical response.

In the next step, in order to find out the critical pressure where such spin-state transition happens for the two compounds, we increased the pressure in step of 0.6-0.7 GPa, starting from the ambient pressure condition. As shown in the plot of the magnetic moment (M) versus pressure (P) in Fig. 3, we find a spin-state from HS with total magnetic moment of  $4 \mu_B/\text{Fe}$  to LS with a total moment of  $0 \mu_B/\text{Fe}$  at pressure ( $P_c \uparrow$ ) of 4.7 GPa for DMAFeF and 6.6 GPa for HAFeF. This implies a strong influence of choice of A cation on the optimal pressure needed for spin-state transition. We then decreased the pressure starting from the highest applied pressure. Interestingly we find the optimal pressure required for the transition from LS with a total moment of  $0 \mu_B/\text{Fe}$  to HS with total magnetic moment of  $4 \mu_B/\text{Fe}$ , happens at a different pressure ( $P_c \downarrow$ ) compared to  $P_c \uparrow$ , having values 2.5 GPa for DMAFeF and 1.4 GPa for HAFeF. There is reflected as significant hysteresis effect in M-P data in case of both compounds, with width of hysteresis being 2.2 GPa for DMAFeF as compared to 5.2 GPa for HAFeF, the former being more than a factor of 2 smaller than the latter. Therefore, the choice of A cation has a significant influence on spin-switching properties. This constitutes the key finding of our investigation. We note that both  $P_c \uparrow$  and  $P_c \downarrow$  are of moderate values for both compounds, that can be generated in a laboratory set-up.

**Microscopic Understanding-** In order to understand the microscopic origin of the quantitative differences in response of the two formate frameworks considered in this study to the applied pressure, we firstly calculated the mechanical strengths of the two compounds. As mentioned previously due to the differential nature of H bonding, the lattice for HAFeF is expected to be

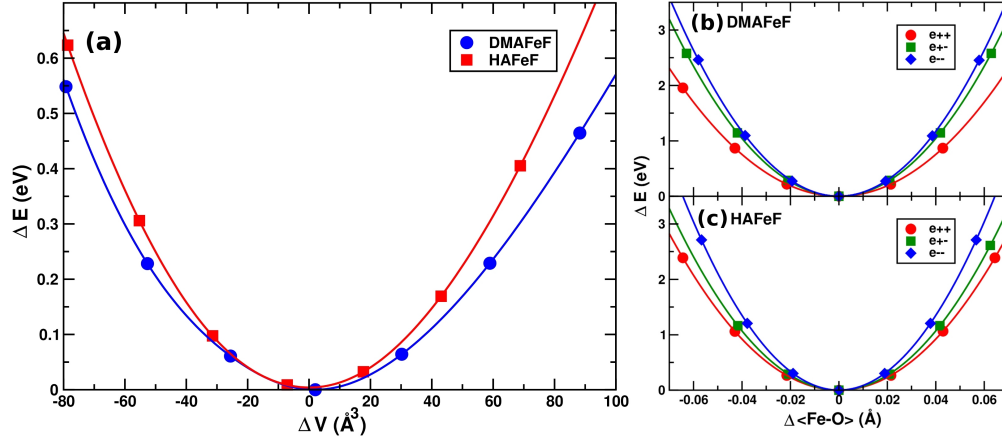


Figure 4: Panel (a): Total energy versus volume of the unit cell for DMAFeF and HAFeF. Energy and volumes have been measured with respect to the equilibrium values,  $E_0$  and  $V_0$ , respectively. The symbols denote the DFT calculated data points and the lines depict the that obtained from fitting with Murnaghan<sup>20</sup> equation of state. Panel (b): The variation of total energy as a function of variation of Fe-O bondlength about the equilibrium value, for different spin-state configurations of neighboring Fe atoms, LS-LS (diamond), LS-HS (square) and HS-HS (circle). Solid lines are fit to the data points. Panel (c): same as in panel (b), but for HAFeF.

more rigid compared to that of DMAFeF. This is confirmed by the magnitudes of the calculated bulk moduli of the two systems. The fit of the DFT total energy versus volume data to the Birch-Murnaghan equation of state,<sup>20</sup> as shown in Fig. 4(a), gave the bulk modulus to be 21.55 GPa for DMAFeF, and 24.27 GPa for HAFeF, with  $B'_0 = 5.39$  and 1.84, respectively. This would in turn imply that the critical pressure needed to cause spin-switching through change in Fe-O bondlength to be larger in the significantly more rigid lattice of HAFeF compared to that in comparatively less rigid lattice of DMAFeF, as reflected in different values of  $P_c \uparrow$  in two compounds.

Further to elucidate the mechanism by which the cooperativity, manifested in form of hysteresis in the M-P plot, develops in these materials we computed the elastic and magnetic exchange interactions. The most prevalent idea in this context attributes the microscopic origin of cooperativity to the elastic interaction between local distortions at the SCO centers.<sup>23</sup> However in a very recent work, the importance of magnetic super-exchanges in driving cooperativity was uncovered.<sup>11</sup> Depending on the sign of the spin-dependent elastic interaction, which is dictated by the nature of the spin-phonon coupling in the material, the magnetic interaction was found to be influence

the hysteresis in a quantitative or qualitative way. As was found in Ref.<sup>11</sup> the interplay between elastic and magnetic interaction in building up cooperativity, crucially relies on the spin-dependent rigidity of the lattice. Depending the spin-state of the spin-crossover ion, which is Fe in the present case, the elastic interaction between two neighboring Fe ions can be different, which are labeled as  $e_{++}$  ( $e_{--}$ ) for both neighboring sites in HS (LS) state, and  $e_{-+}$  for one site in LS and another in HS. The size change of the SCO unit upon change of spin-state makes  $e_{--} > e_{++}$ . It is thus the value of  $e_{-+}$  which decides the nature (sign) of the effective elastic interaction. Following the work by K Boukheddaden et al.,<sup>23</sup> the effective elastic interaction between two neighboring SCO sites is given by,

$$K = \frac{1}{8} \ln\left(\frac{e_{+-}^2}{e_{++} \times e_{--}}\right)$$

Thus the effective elastic interaction,  $K$  turns out to be of ferroelastic nature for  $e_{+-} > \sqrt{e_{++} \times e_{--}}$  and of antiferroelastic nature for  $e_{+-} < \sqrt{e_{++} \times e_{--}}$ . It was demonstrated<sup>11</sup> that for ferro type elastic interaction, the magnetic interaction becomes operative only in qualitative manner, in terms of enhancing the hysteresis width, while for antiferro nature of elastic interaction, the magnetic exchange is the sole driving force in setting up the hysteresis.

In order to have a microscopic understanding of the observed hysteresis in M-P plot of the studied formate frameworks and its dependence on the choice of the amine cation, we thus first calculated the spin-state dependent elastic interactions for the two compounds. To do so, we adopted the same procedure as in Ref.<sup>11</sup> Electronic structure of the optimized crystal structure data shows that the LS state is obtained at a high pressure phase for an average Fe-O bond length of 1.9 Å<sup>0</sup> or less, while the HS state is obtained at an ambient pressure phase for for an average Fe-O bond length of 2.1 Å<sup>0</sup> or more. Keeping this in mind, we constructed crystal structures setting the average Fe-O bond length at 1.9 and 2.1 Å<sup>0</sup> to emulate the LS and HS states of neighboring Fe-O<sub>6</sub> octahedra, respectively. To simulate the LS-HS situation, structure with alternating arrangements of Fe-O<sub>6</sub> octahedra having average Fe-O bond lengths of 1.9 and 2.2 Å<sup>0</sup> was constructed. Considering the three model structures with HS-HS, LS-LS and LS-HS arrangements of neighboring Fe-O<sub>6</sub> octahedra, the Fe-O bond lengths were varied by small amounts ( $\approx 0.02 - 0.06$ ) within the

harmonic oscillation limit around the equilibrium bond lengths. The obtained energy versus bond length variation for the three cases for both the compounds are shown in Figs. 4(b) and (c). A parabolic fit of the data points provides the estimates of the spin-dependent elastic interactions. DMAFeF is found to be weakly ferroelastic with  $e_{+-} \simeq \sqrt{e_{++} \times e_{--}}$  while HAFeF is found to be strongly ferroelastic with  $e_{+-} > \sqrt{e_{++} \times e_{--}}$ , having effective elastic constant of 3.52 K for DMAFeF compared to a substantially larger effective elastic constant of 8.93K for HAFeF.

We next turn on to the magnetic super-exchange coupling between neighboring Fe(II) centers in HS state. To estimate their values we calculated the total energies of ferromagnetic and antiferromagnetic Fe<sup>2+</sup> spin configurations, and mapped on to the spin Hamiltonian

$$\mathcal{H}_{magnetic} = J \times S_i \times S_j$$

, where  $J$  is the magnetic exchange between nearest neighbor Fe<sup>2+</sup> spins,  $S_i$  and  $S_j$ . The difference of the ferromagnetic and antiferromagnetic energies provides the estimate of  $J$ , which turned out to be of antiferromagnetic for the compounds, and of values 3.19K for DMAFeF and 2.85K for HAFeF. This leads us to conclude that while the magnetic exchanges in the two compounds are of same sign and of similar strengths, the spin-dependent elastic interactions are of ferroelastic nature with significantly larger strength for HAFeF compared to DMAFeF. Following the previous literature<sup>11</sup> we also conclude that primary responsible factor in driving cooperativity in these formate frameworks is the spin-dependent lattice effect, helped by the magnetic exchange. This is different from the case of coordination polymer compounds in which it was found to be entirely driven by the magnetic super-exchanges.<sup>11,24</sup> The change of amine cation, leads to the change in cross-linking hydrogen bonding, and thus to the rigidity of the lattices. Interestingly, the change of amine molecule is also found to effect the spin-phonon coupling, thereby producing a profound effect on the cooperativity.

## Conclusions

In summary, we show that apart from exhibiting interesting multiferroic properties transition metal formate based hybrid perovskites are also potential candidates for exhibiting spin-switching upon application of external stimuli. We demonstrated this through rigorous first-principles calculations, considering two formate based hybrid perovskite compounds, DMAFeF and HAFeF under hydrostatic pressure. We found that dense framework structures of these compound help in building up cooperativity in spin-switching, making the phenomena a spin-state transition with appreciable hysteresis effect. The spin-switching is reflected in associated changes in electronic, magnetic and also possible changes in optical properties. This opens up several novel potential applications of these materials, for example, as pressure sensors, as active elements of various types of displays, and in information storage and retrieval - an aspect which has remained unexplored so far. Our computed values of pressure needed to drive the spin-state transition is found to be in the range of about 2-6 GPa, which should be readily achievable in a laboratory set-up of a low to medium pressure diamond anvil cell (DAC). The appreciable hysteresis effect of 2-5 GPa associated with these spin-state transitions would make them functional in memory devices for a reasonably wide range of pressure. Interestingly, taking the advantage of flexibility of these MOF perovskites to undergo substantial change in mechanical properties upon tuning of hydrogen bonds, both the pressure required from the transition, as well as the hysteresis-width are found to be tunable by choice of appropriate amine cation. Investigation of microscopies shows elastic properties are vastly different between the two studied compounds, lending support to our observation.

While in our study, we considered only a particular type of external perturbation, namely the hydrostatic pressure, in principle such SCO in hybrid perovskites may occur upon light irradiation, or by application of magnetic field, as observed in many of the metal-organic complexes.<sup>25</sup> Light induced spin-switching, if can be achieved in hybrid perovskites, will make these materials useful in application as optical switches as well as for studying phenomena as light-induced excited spin-state trapping. We hope that our study will stimulate further research, both experimental and theoretical, in discovering this new aspect of hybrid perovskites.

# Supporting Information

The computed structures of DMAFeF and HAFeF, provided as .cif files.

## Acknowledgement

H.B and T.S.D acknowledge the computational support of Thematic Unit of Excellence on Computational Materials Science, funded by Nano-mission of Department of Science and Technology.

## References

- (1) Kieslich, G.; Sun, S.; Cheetham, A. K. Solid-state principles applied to organic-inorganic perovskites: new tricks for an old dog. *Chem. Sci.*, **2014**, 5, 4712.
- (2) Shekhah, O.; Liu, J.; Fischer, R. A.; Wöll, Ch. MOF thin films: existing and future applications. *Chem. Soc. Rev.*, **2011**, 40, 1081-1106.
- (3) Li, B.; Wen, H. M.; Zhou, W.; Chen, B. Porous Metal-Organic Frameworks for Gas Storage and Separation: What, How, and Why? *J. Phys. Chem. Lett.*, **2014**, 5 (20), 3468-3479
- (4) Kreno, L. E.; Leong, K.; Farha, O. K.; Allendorf, M.; van Duyne, R. P.; Hupp, J. T. Metal-Organic Framework Materials as Chemical Sensors. *Chem. Rev.*, **2012**, 112 (2), 1105-1125
- (5) Ranocchiari, M.; van Bokhoven, J. A. Catalysis by metal-organic frameworks: fundamentals and opportunities. *Phys. Chem. Chem. Phys.*, **2011**, 13, 6388-6396
- (6) Tejuca, L.; Fierro, J. *Properties and Applications of Perovskite-Type Oxides*, CRC Press, New York, 1993.
- (7) Yin, W-J.; Yang, J-H.; Kang, J.; Yan, Y.; Wei, S-H. Halide perovskite materials for solar cells: a theoretical review. *J. Mater. Chem. A*, **2015**, 3, 8926.
- (8) Jain, P.; Ramachandran, V.; Clark, R. J.; Zhou, H. D.; Toby, B. H.; Dalal, N. S.; Kroto, H. W.; Cheetham, A. K. Multiferroic Behavior Associated with an Order-Disorder Hydrogen Bonding Transition in Metal-Organic Frameworks (MOFs) with the Perovskite ABX<sub>3</sub> Architecture. *J. Am. Chem. Soc.* **2009**, 131, 13625-13627.
- (9) Liu, S.; Cohen, R. E. Response of Methylammonium Lead Iodide to External Stimuli and Caloric Effects from Molecular Dynamics Simulations. *J. Phys. Chem. C*, **2016**, 120 (31), 17274-17281.

- (10) Li, W.; Thirumurugan, A.; Barton, P. T.; Lin, Z.; Henke, S.; Yeung, H. H-M.; Wharmby, M. T.; Bithell, E. G.; Howard, C. J.; Cheetham, A. K. Mechanical Tunability via Hydrogen Bonding in Metal-Organic Frameworks with the Perovskite Architecture. *J. Am. Chem. Soc.*, **2014**, 136, 7801-7804.
- (11) Banerjee, H.; Kumar, M.; Saha-Dasgupta, T. Cooperativity in spin-crossover transition in metalorganic complexes: Interplay of magnetic and elastic interactions. *Phys. Rev B.*, **2014**, 90, 174433.
- (12) Kahn, O.; Kröber, J.; Jay, C. Spin Transition Molecular Materials for displays and data recording. *Adv. Mat.*, **1992**, 4(11), 718-728.
- (13) Kahn, O.; Martinez, C. J. Spin-Transition Polymers: From Molecular Materials Toward Memory Devices. *Science*, **1998**, 279(5347), 44-48.
- (14) Li, N.; Manoun, B.; Tang, L.; Ke, F.; Liu, F.; Dong, H.; Lazor, P.; Yang, W. Pressure-Induced Structural and Electronic Transition in Sr<sub>2</sub>ZnWO<sub>6</sub> Double Perovskite. *Inorg. Chem.*, **2016**, 55 (13), 6770-6775
- (15) Kresse, G.; Hafner, J. Ab initio molecular dynamics for liquid metals. *Phys. Rev. B (R)*, **1993**, 47, 558.
- (16) Kresse, G.; Furthmüller, J. Efficient iterative schemes for ab initio total-energy calculations using a plane-wave basis set. *Phys. Rev. B*, **1996**, 54, 11169.
- (17) Blöchl, P. E. Projector augmented-wave method. *Phys. Rev. B*, **1994** 50, 17953.
- (18) Perdew, J. P.; Burke, K.; Ernzerhof, M. Generalized Gradient Approximation Made Simple. *Phys. Rev. Lett.*, **1996**, 77, 3865.
- (19) Liechtenstein, A.I.; Anisimov, V. I.; Zaanen, J. Density-functional theory and strong interactions: Orbital ordering in Mott-Hubbard insulators. *Phys. Rev. B (R)*, **1995**, 52, R5467.
- (20) Murnaghan, F. D.; The Compressibility of Media under Extreme Pressures. *Proceedings of the National Academy of Sciences of the United States of America*, **1944**, 30 (9), 244-247
- (21) Sanchez-Andujar, M.; Presedo, S.; Yanez-Vilar, S.; Castro-Garcia, S.; Shamir, J.; Senaris-Rodriguez, M.A. Characterization of the order-disorder dielectric transition in the hybrid organic-inorganic perovskite-like formate Mn(HCOO)<sub>3</sub>[(CH<sub>3</sub>)<sub>2</sub>NH<sub>2</sub>]. *Inorganic Chemistry*, **2010** 49, (4) 1510-1516
- (22) Liu, B.; Shang, R.; Hu, K-L.; Wang, Z-M.; Gao, S. A New Series of Chiral Metal Formate Frameworks of [HONH<sub>3</sub>][M<sup>II</sup>(HCOO)<sub>3</sub>] (M = Mn, Co, Ni, Zn, and Mg): Synthesis, Structures, and Properties. *Inorg. Chem.*, **2012**, 51 (24), 13363-13372.

- (23) Boukheddaden, K.; Miyashita, S.; Nishino, M. Elastic interaction among transition metals in one-dimensional spin-crossover solids. *Phys. Rev. B*, **2007** 75, 094112.
- (24) Jeschke, H. O.; Salguero, L. A.; Rahaman, B.; Buchsbaum, C.; Pashchenko, V.; Schmidt, M. U.; Saha-Dasgupta, T.; Valenti, R. Microscopic modeling of a spin crossover transition. *New Journal of Physics*, **2007**, 9, 448.
- (25) Gütlich, Philipp; Gaspar, Ana. B; Garcia, Yann. Spin state switching in iron coordination compounds. *Beilstein J. Org. Chem.*, **2013**, 9, 342.